

A SCHWARTZ-CHRISTOFFEL ANALYSIS OF CAVITATING FLOW IN A
TWO-DIMENSIONAL MITERED ELBOW

by

JOHN WILLIAM HYDEN

A THESIS

submitted to

OREGON STATE COLLEGE

in partial fulfillment of
the requirements for the
degree of

MASTER OF SCIENCE

June 1961

APPROVED:

Redacted for Privacy

Associate Professor of Civil Engineering

In Charge of Major

Redacted for Privacy

Head of Department of Civil Engineering

Redacted for Privacy

Chairman of School Graduate Committee

Redacted for Privacy

Dean of Graduate School

Date thesis is presented May 31, 1960

Typed by Mrs. Selma R. Dingus

ACKNOWLEDGEMENTS

In addition to making an analysis of a two-dimensional mitered elbow using the Schwartz-Christoffel Transformation and testing this analysis by actual laboratory experiment, it was necessary to be oriented in basic complex variables and their application to the Schwartz-Christoffel Transformation. The author wishes to express his appreciation to Dr. Charles E. Behlke for his instruction in complex variables and in the Schwartz-Christoffel Transformation. Before this thesis was completed however, Dr. Behlke left Oregon State College for post doctoral study under a National Science Foundation Faculty Fellowship, and Dr. Roy H. Shoemaker became the author's major professor. The author therefore greatly appreciates Dr. Shoemaker's as well as Dr. Behlke's advice and encouragement in the writing of this thesis. Also very much appreciated was Mr. Edwin M. Bryan's able assistance in setting up the laboratory apparatus.

TABLE OF CONTENTS

	Page
Introduction and Purpose	1
The Schwartz-Christoffel Transformation	2
General Orientation	2
Derivation of Equations	5
Explanation of Terms	11
Laboratory Analysis	16
Laboratory Apparatus	16
Procedure	19
Calculation of Terms	21
Experimental Results	21
Conclusions	24
Bibliography	28

APPENDICES

Appendix

A	Relation of Velocity Ratios to Euler Numbers	29
B	Finding Values of z , Velocity Ratios, and Euler Numbers Using the Schwartz-Christoffel Transformation Equations	30
C	Laboratory Results	32
D	Reynolds Number Calculations	36

LIST OF ILLUSTRATIONS

	Page
Figure 1 Schematic Diagrams of the z, t, and w Planes	4
Figure 2 Coordinates, Exterior Angles, and Flow Directions for the z, t, and w Planes Used in this Analysis	6
Figure 3 Equipotential Lines Plotted against Their Location	14
Figure 4 Equipotential Lines Plotted against Euler Numbers of the Point in Question	15
Figure 5 Schematic Diagram of the Laboratory Test Section Used for the March 9 and March 23, 1960 Tests	17
Figure 6 Schematic Diagram of the Laboratory Test Section Used for the July, 1959 Tests	18
Figure 7 Overall Schematic Diagram of the Laboratory Apparatus	20

LIST OF TABLES

Table 1 Location of the Given Equipotential Lines, and Velocity Ratios and Euler Numbers at the Given Points	13
Table 2 Summary of Experimental Results	22

A SCHWARTZ-CHRISTOFFEL ANALYSIS OF CAVITATING FLOW IN A TWO-DIMENSIONAL MITERED ELBOW

INTRODUCTION AND PURPOSE

Cavitation is a phenomenon commonly found in hydraulic machines and pipe systems. It exists where there are high localized velocities, or else where there is a high enclosed elevation head such as may be found in vertical draft tubes. These high velocities or high elevations will induce low pressures in a fluid, and may decrease the pressure until vapor pressure is reached, at which point vapor pockets form. These vapor pockets are carried downstream to points of higher pressure where they collapse.

Because the vapor cavities reduce the area available for fluid flow, cavitation will reduce the efficiency of hydraulic machinery considerably. In addition, the formation and collapse of vapor pockets will cause stress reversals in various parts of hydraulic machinery and conduit systems. Ship propellers and turbine runners have been severely damaged due to cavitation. Concrete penstocks in which high local velocities exist have been literally eroded away by cavitation-induced shock waves. Cavitation has usually been avoided by proper design and thus elimination of these high localized velocities.

A ninety degree elbow has a very high velocity at the inside corner compared to the average velocity which exists

in the straight section upstream or downstream from the corner. It is because of this high relative velocity that cavitation can exist at the inside corner of a ninety degree elbow. The purpose of this thesis is to perform an analysis of the flow pattern in which cavitation is present rather than suggest any design practices which should be followed in order to eliminate cavitation.

The analysis consists of determining mathematically the flow net in a ninety degree mitered elbow and then considering its validity, when cavitation is occurring, by actual laboratory experiment.

THE SCHWARTZ-CHRISTOFFEL TRANSFORMATION

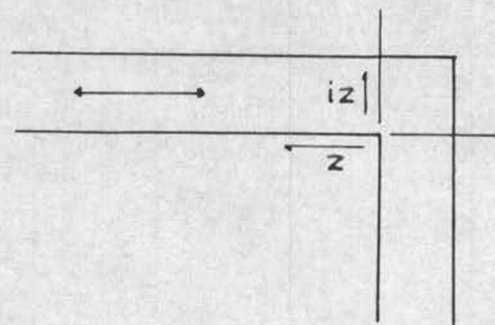
General Orientation

The mathematical analysis to be used in this presentation is the Schwartz-Christoffel Transformation. The Schwartz-Christoffel Transformation as applied to fluid flow assumes that fluid will flow around any polygon or boundary shape without separation. For some boundary shapes that do not have abrupt changes, this transformation is undoubtedly valid. For some sections of a ninety degree elbow upstream from the corner, the actual fluid flow follows the ideal conditions assumed in the Schwartz-Christoffel Transformation. At the points where it exists, cavitation certainly

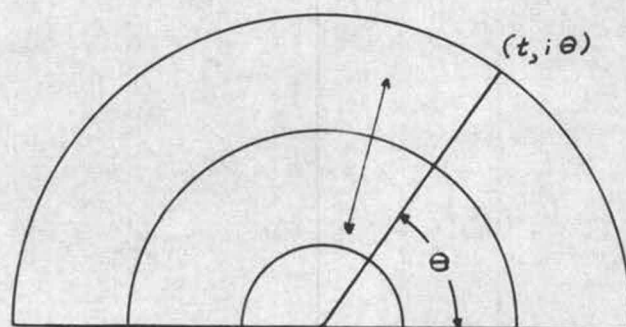
produces a different pressure distribution from that realized in noncavitating flow. The purpose of testing the flow in a ninety degree elbow when cavitation is present was to see if the flow at the inside boundary slightly upstream from the corner followed the ideal conditions as presented in the Schwartz-Christoffel Transformation.

The transformation involves the establishment of a flow net for the channel in question by transferring points into the flow net, or real plane, from a simple flow net, which is made up of a grid of perfect squares, and which is located on a separate imaginary plane. The analysis is made as simple as possible by two methods: first, the transformation is two-dimensional, and second, because it is necessary only to find the velocity distribution near the inside corner of the elbow, only the segments of the flow net along the inside boundary are determined.

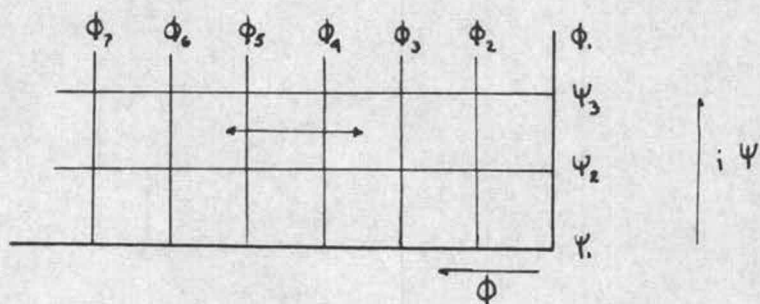
This particular analysis involves the use of three planes: the z plane, which is the real plane of the two-dimensional elbow itself, the t plane, which is an intermediate plane, and the w plane, which is the final imaginary plane described in the preceding paragraph. These planes are shown schematically in Figure 1.



z Plane



t Plane



w Plane

Figure 1

Schematic Diagrams of the z , t , and w Planes

The z and w planes have rectangular complex coordinates; the t plane, polar complex coordinates. The two-headed arrows indicate the directions in which flow can occur on each plane. The specific points and flow directions for this problem are established as shown in Figure 2.

Derivation of Equations

The general form of the Schwartz-Christoffel Transformation is $z = A \left[\int (t-a)^{-\frac{\alpha}{\pi}} (t-b)^{-\frac{\beta}{\pi}} (t-c)^{-\frac{\gamma}{\pi}} \dots dt \right] + B$ where $[a, b, c, \dots]$ are points on the t plane, and $[\alpha, \beta, \gamma, \dots]$ are exterior angles of the real polygon. The algebraic summation of these angles is, of course, 2π . (Reference 1, p. 173)

The derivation of the transformation from the z plane to the t plane is as follows:

$$z = A \left[\int (t-a)^{-\frac{\alpha}{\pi}} (t-b)^{-\frac{\beta}{\pi}} (t-c)^{-\frac{\gamma}{\pi}} (t-d)^{-\frac{\delta}{\pi}} dt \right] + B$$

$$a = 0 \quad b = -1 \quad c = \infty \quad d = +1$$

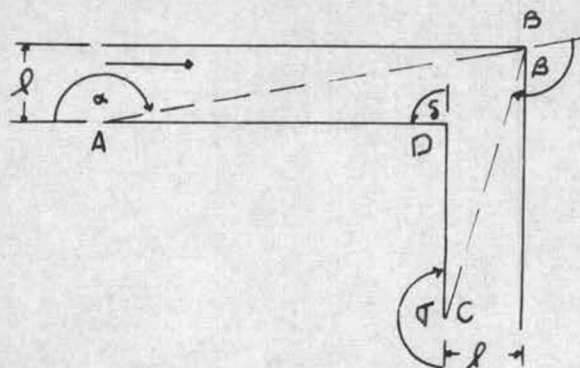
$$\alpha = \pi \quad \beta = \frac{\pi}{2} \quad \gamma = \pi \quad \delta = -\frac{\pi}{2}$$

$$z = A \left[\int (t^{-1}) (t+1)^{-1/2} (t-1)^{1/2} dt \right] + B$$

$$= A \left[\int \left(\frac{1}{t} \cdot \frac{t-1}{\sqrt{t^2-1}} \right) dt \right] + B = A \left[\int \left(\frac{dt}{\sqrt{t^2-1}} - \frac{dt}{t \sqrt{t^2-1}} \right) \right] + B$$

$$= A \left[\ln (t + \sqrt{t^2-1}) - \cos^{-1} \frac{1}{t} \right] + B$$

$$\ln (t + \sqrt{t^2-1}) = \ln \left| t + \sqrt{t^2-1} \right| + i \arg (t + \sqrt{t^2-1})$$

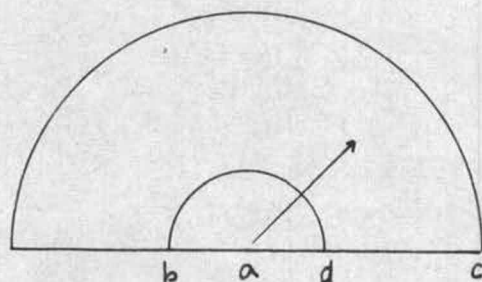


z Plane

Coordinates	Exterior Angles
-------------	-----------------

A $\infty, i0$	$\alpha = \pi$
B $-l, il$	$\beta = \frac{\pi}{2}$
C $0, -i\infty$	$\gamma = \pi$
D $0, i0$	$\delta = -\frac{\pi}{2}$

Flow is from A to C

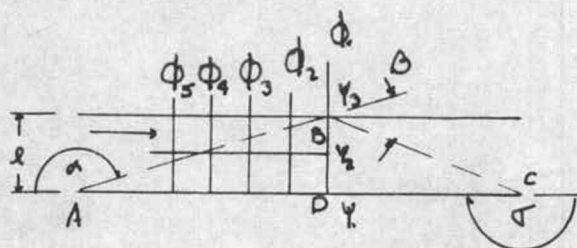


t Plane

Coordinates

a $0, 0$
b $-1, 0$
c $\infty, 0$
d $1, 0$

Flow is from Source a



w Plane

Coordinates	Exterior Angles
-------------	-----------------

A $-\infty, i0$	$\alpha = \pi$
B $0, il$	$\beta = 0$
C $\infty, i0$	$\gamma = \pi$
D $0, 0$	$\delta = 0$

Flow is from A to C

Figure 2

Coordinates, Exterior Angles, and Flow Directions for the z, t, and w Planes Used in this Analysis

$$\text{Let } \cos^{-1} \frac{1}{t} = u$$

$$\cos u = \frac{e^{iu} + e^{-iu}}{2} = \frac{1}{t}$$

$$e^{iu} + e^{-iu} = \frac{2}{t}$$

$$e^{2iu} + 1 = \frac{2e^{iu}}{t}; e^{2iu} - \frac{2e^{iu}}{t} + 1 = 0$$

$$e^{iu} = \frac{\frac{2}{t} \pm \sqrt{\frac{4}{t^2} - 4}}{2} = \frac{\frac{2}{t} \pm 2\sqrt{\frac{1}{t^2} - 1}}{2} = \frac{1}{t} \pm \sqrt{\frac{1}{t^2} - 1}$$

$$iu = \ln \left(\frac{1}{t} \pm \sqrt{\frac{1}{t^2} - 1} \right) \quad \text{and}$$

$$u = \frac{\ln \left(\frac{1}{t} \pm \sqrt{\frac{1}{t^2} - 1} \right)}{i} = -i \ln \left(\frac{1}{t} \pm \sqrt{\frac{1}{t^2} - 1} \right)$$

$$= -i \ln \left| \frac{1}{t} \pm \sqrt{\frac{1}{t^2} - 1} \right| + \arg \left(\frac{1}{t} \pm \sqrt{\frac{1}{t^2} - 1} \right)$$

$$z = A \left[\ln \left| t + \sqrt{t^2 - 1} \right| + i \arg (t + \sqrt{t^2 - 1}) \right. \\ \left. + i \ln \left| \frac{1}{t} \pm \sqrt{\frac{1}{t^2} - 1} \right| - \arg \left(\frac{1}{t} \pm \sqrt{\frac{1}{t^2} - 1} \right) \right] + B$$

Using the plus sign in $\frac{1}{t} \pm \sqrt{\frac{1}{t^2} - 1}$ and setting $t = 1$

then from Figure 2, $z = 0 + i0$.

$$z = A \left[\ln |1| + i \arg (1) + i \ln \left| 1 \right| - \arg (1) \right] + B \\ = A [0 + i0 + i0 - 0] + B$$

$$0 = A(0) + B \quad B = 0$$

Setting $t = -1$, and again from Figure 2, $z = -\ell + i\ell$

$$z = -\ell + i\ell = A \left[\ln |-1| + i \arg(-1) + i \ln |-1| - \arg(-1) \right]$$

$$= A \left[0 + i\pi + 0 - \pi \right]$$

$$A = \frac{-\ell + i\ell}{-i\pi + i\pi} = \frac{\ell}{\pi}$$

$$z = \frac{\ell}{\pi} \left[\ln \left| t + \sqrt{t^2 - 1} \right| + i \arg(t + \sqrt{t^2 - 1}) + i \ln \left| \frac{1}{t} + \sqrt{\frac{1}{t^2} - 1} \right| - \arg\left(\frac{1}{t} + \sqrt{\frac{1}{t^2} - 1}\right) \right] \quad (\text{Equation 1})$$

The next step is to obtain a transformation from the t plane to the w plane. Referring to Figure 2, this transformation consists of the analysis of an infinite strip units wide. (Reference 1, p. 177) The derivation follows.

$$w = \phi + i\psi = A \left[\int (t-a)^{-\frac{\alpha}{\pi}} (t-b)^{-\frac{\beta}{\pi}} (t-c)^{-\frac{\sigma}{\pi}} (t-d)^{-\frac{\delta}{\pi}} dt \right] + B$$

$$a = 0 \quad b = -1 \quad c = \infty \quad d = +1$$

$$\alpha = \pi \quad \beta = 0 \quad \sigma = \pi \quad \delta = 0$$

$$w = A \left[\int (t^{-1}) (t+1)^0 (t-1)^0 dt \right] + B$$

$$= A \int \frac{dt}{t} + B = A \ln t + B$$

Setting $t = 1$; from Figure 2, $w = 0 + i0$

$$0 + i0 = A \ln(1) + B = A(0) + B \quad B = 0$$

Setting $t = -1$; again from Figure 2, $w = 0 + i$

$$0 + i\ell = A \ln(-1) = A(i\pi) \quad A = \frac{i\ell}{i\pi} = \frac{\ell}{\pi}$$

$$w = \phi + i\psi = -\ln t$$

$$\ln t = \frac{\pi(\phi + i\psi)}{\ell} \quad e^{\frac{(\phi + i\psi)}{\ell}} = t$$

Along the inside boundary of the elbow (from point A to D), $\psi = 0$. The transformation for the elbow along the inside boundary becomes

$$t = e^{\frac{\pi \phi}{\ell}} \quad (\text{Equation 2})$$

Velocity equals $\frac{dw}{dz} = \frac{dt}{dz} \cdot \frac{dw}{dt}$

$$\frac{dz}{dt} = \frac{\ell}{\pi} \left[\frac{1}{t} \sqrt{\frac{t-1}{t+1}} \right] \quad \text{and} \quad \frac{dt}{dz} = \frac{\pi}{\ell} \left[t \sqrt{\frac{t+1}{t-1}} \right]$$

$$\frac{dw}{dt} = \frac{\ell}{\pi} \left(\frac{1}{t} \right) \quad (\text{Equation A})$$

$$\frac{dw}{dz} = \frac{dw}{dt} \cdot \frac{dt}{dz} = \sqrt{\frac{t+1}{t-1}} = \sqrt{\frac{e^{\frac{\pi \phi}{\ell}} + 1}{e^{\frac{\pi \phi}{\ell}} - 1}}$$

From Figure 1, ϕ increases in the upstream direction, and as $e^{\frac{\pi \phi}{\ell}} \rightarrow \infty$ then

$$\frac{dw}{dz} = \sqrt{\frac{e^{\frac{\pi \phi}{\ell}} + 1}{e^{\frac{\pi \phi}{\ell}} - 1}} \quad \text{approaches 1}$$

If Q is the flow per unit width of elbow and q_0 is the velocity where there is uniform flow, then $Q = \ell q_0$. Also,

$$\frac{dw}{dz} \text{ upstream} = q_0 = q_0 \sqrt{\frac{\frac{\pi\phi}{\ell}}{e^{\frac{\pi\phi}{\ell}} + 1}} \quad (\text{Equation 3})$$

$$\text{and } \frac{dw}{dt} = \frac{\ell}{\pi} \cdot \frac{q_0}{t} \quad (\text{Note Equation A, page 9})$$

$$w = \frac{\ell q_0}{\pi} \ln t = \frac{Q}{\pi} \ln t$$

$$\ln t = \frac{\pi w}{Q} = \frac{\pi\phi}{Q} \quad \text{for this case}$$

Equation 2 becomes

$$t = e^{\frac{\pi\phi}{Q}} \quad (\text{Equation 2-A})$$

Also Equation 1 becomes

$$z = \frac{\ell}{\pi} \left[\ln \left| \frac{\pi\phi}{e^{\frac{\pi\phi}{Q}}} + \sqrt{\frac{2\pi\phi}{e^{\frac{\pi\phi}{Q}} - 1}} \right| + i \arg \left(e^{\frac{\pi\phi}{Q}} + \sqrt{\frac{2\pi\phi}{e^{\frac{\pi\phi}{Q}} - 1}} \right) \right. \\ \left. + i \ln \left| e^{\frac{-\pi\phi}{Q}} + \sqrt{\frac{-2\pi\phi}{e^{\frac{-\pi\phi}{Q}} - 1}} \right| - \arg \left(e^{\frac{-\pi\phi}{Q}} + \sqrt{\frac{-2\pi\phi}{e^{\frac{-\pi\phi}{Q}} - 1}} \right) \right] \quad (\text{Equation 1-A})$$

Equation 3 becomes

$$\frac{dw}{dz} = q_0 \sqrt{\frac{\frac{\pi\phi}{Q}}{e^{\frac{\pi\phi}{Q}} + 1}} \quad (\text{Equation 3-A})$$

If V_1 equals q_0 and V_2 equals the local downstream velocity near the corner, then $\frac{V_2}{V_1} = \sqrt{\frac{\frac{\pi\phi}{Q} + 1}{\frac{\pi\phi}{Q} - 1}}$

The Euler Number is next found in terms of the velocity ratio $\frac{V_2}{V_1}$. As shown in Appendix A,

$$\frac{1}{\sqrt{\left(\frac{V_2}{V_1}\right)^2 - 1}} = \frac{V_1}{\sqrt{2\Delta p/\rho}} \quad \text{Euler Number (Equation 4)}$$

The Euler Numbers determined from Equation 4 are compared with those obtained from actual laboratory experiment to determine the validity of the Schwartz-Christoffel Transformation. Euler Numbers are used in preference to velocity ratios as pressure readings and average velocities were obtained in the laboratory analysis.

Explanation of Terms

On the following pages, values of $\frac{\phi}{Q}$, z , $\frac{dw}{dz} \cdot \frac{1}{q_0}$, and Euler Numbers are tabulated and plotted. These terms will now be discussed in detail. Q is the flow per unit width of elbow and q_0 is the velocity where uniform flow exists. ϕ represents the equipotential lines and $\frac{\phi}{Q}$ is the convenient

form for this representation. z , which is the location of the equipotential lines, is based on Equation 1-A which is

$$z = \frac{\ell}{\pi} \left[\ln \left| e^{\frac{\pi\phi}{Q}} + \sqrt{e^{\frac{2\pi\phi}{Q}} - 1} \right| + i \arg \left(e^{\frac{\pi\phi}{Q}} + \sqrt{e^{\frac{2\pi\phi}{Q}} - 1} \right) \right. \\ \left. + i \ln \left| e^{\frac{-\pi\phi}{Q}} + \sqrt{e^{\frac{-2\pi\phi}{Q}} - 1} \right| - \arg \left(e^{\frac{-\pi\phi}{Q}} + \sqrt{e^{\frac{-2\pi\phi}{Q}} - 1} \right) \right]$$

For values of $\frac{\phi}{Q}$ used, $\left(e^{\frac{\pi\phi}{Q}} + \sqrt{e^{\frac{2\pi\phi}{Q}} - 1} \right)$ is not a complex number, and so there is no problem involved in the calculation of the absolute value. Because it is not a

complex number, $\arg \left(e^{\frac{\pi\phi}{Q}} + \sqrt{e^{\frac{2\pi\phi}{Q}} - 1} \right)$ is zero. The

absolute value of $\left(e^{\frac{-\pi\phi}{Q}} + \sqrt{e^{\frac{-2\pi\phi}{Q}} - 1} \right)$ equals one for all

values of $\frac{\phi}{Q}$ used in this analysis, so $\ln \left| e^{\frac{-\pi\phi}{Q}} + \sqrt{e^{\frac{-2\pi\phi}{Q}} - 1} \right|$

is zero. Solution for z therefore involves finding values

only for the first and last terms of the equation. $\frac{dw}{dz} \cdot \frac{1}{q_0}$

is the ratio of velocity at the equipotential line in

question to that upstream where uniform flow is assumed to

exist. As shown in the derivation of Schwartz-Christoffel

TABLE I

LOCATION OF THE GIVEN EQUIPOTENTIAL LINES,
AND VELOCITY RATIOS AND EULER NUMBERS
AT THE GIVEN POINTS

$\frac{\phi}{Q}$	z (inches)	$\frac{dw}{dz} \cdot \frac{l}{q_0}$	Euler Number
0.00955	0.00309	8.1593	0.124
0.01910	0.00889	5.7760	0.176
0.03813	0.01895	4.4734	0.230
0.09549	0.09852	2.5915	0.416
0.1910	0.27710	1.8528	0.638
0.3813	0.58999	1.4710	0.925
0.9549	2.76474	1.0512	3.02
0.1146	0.12987	2.37	0.465

Note: For the laboratory apparatus, the downstream piezometer is 0.13 inches upstream from the corner. Using z equal to 0.13, find $\frac{\phi}{Q}$ of 0.13 from the plot of equipotential lines against z. From plot of $\frac{\phi}{Q}$ against Euler Numbers, find an Euler Number of 0.50 for $\frac{\phi}{Q}$ equal to 0.13. As shown above, finding $\frac{\phi}{Q}$ for z equal to 0.13 by trial and error yields a velocity ratio of 2.37 and an Euler Number of 0.465.

Figure 3

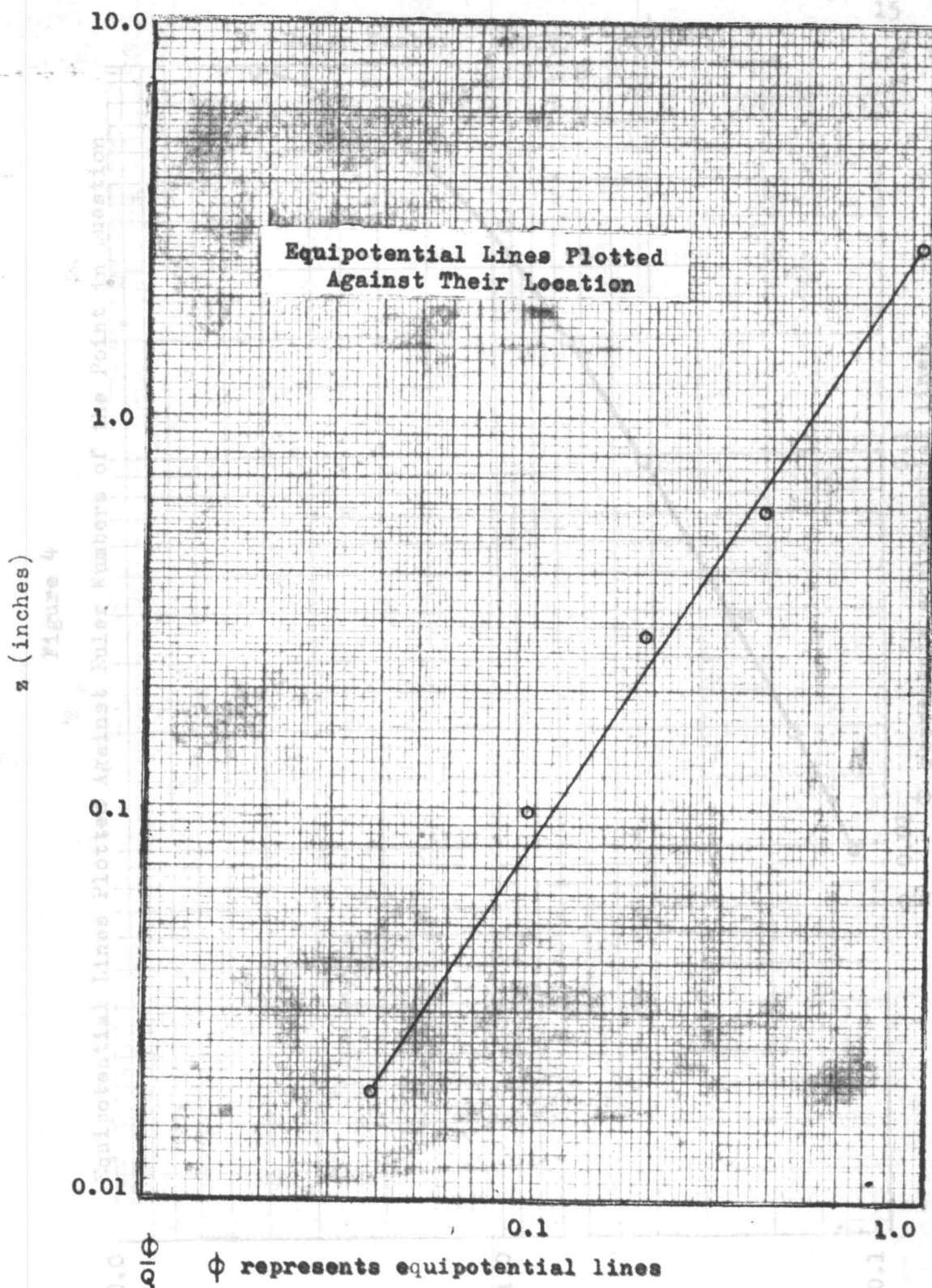
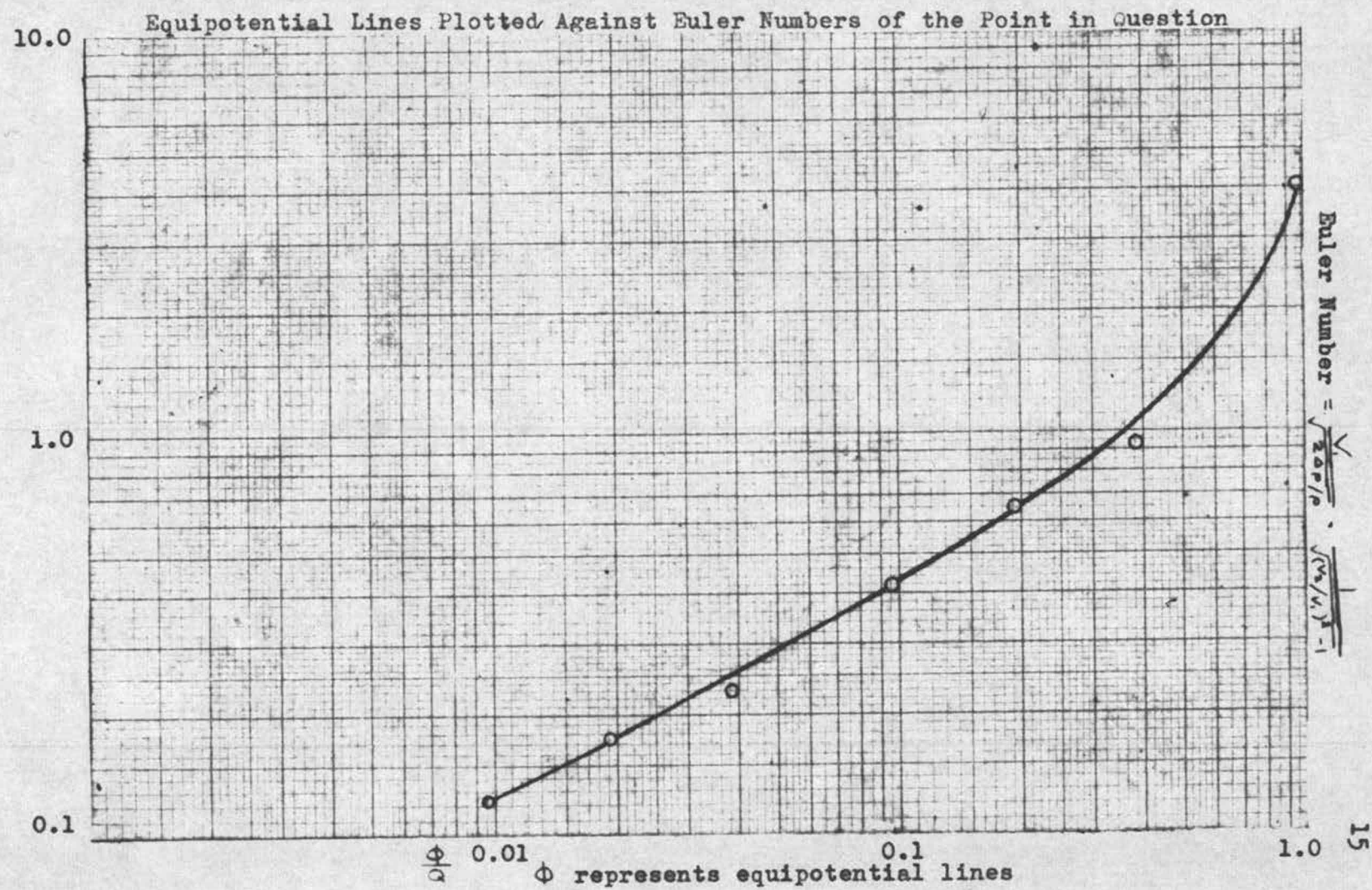


Figure 4



equations

$$\frac{V_2}{V_1} = \sqrt{\frac{\frac{\pi\phi}{Q} + 1}{\frac{\pi\phi}{Q} - 1}} = \frac{dw}{dz} \cdot \frac{1}{q_0} \quad \text{and Euler Number equals } \frac{1}{\sqrt{\left(\frac{V_2}{V_1}\right)^2 - 1}}$$

LABORATORY ANALYSIS

Laboratory Apparatus

The laboratory test section consisted of a four-inch square plexiglas pipe mitered into a ninety degree elbow as shown in Figure 5. The upstream leg was approximately five feet long. The downstream section, about a foot long, was connected to a fifteen foot vertical draft tube which induced cavitation at the inside corner of the elbow. Piezometer taps, one located very close to the inside corner, and the other about a foot upstream where uniform flow was assumed to exist, were connected to a differential manometer. The upstream tap was also connected to an open end manometer so that absolute pressures at both points could be determined. An alternate position for the downstream tap was two inches downstream from the inside corner where the longitudinal pressure distribution was more uniform. In Figure 6 is shown the test section used in the July, 1959 tests. This test

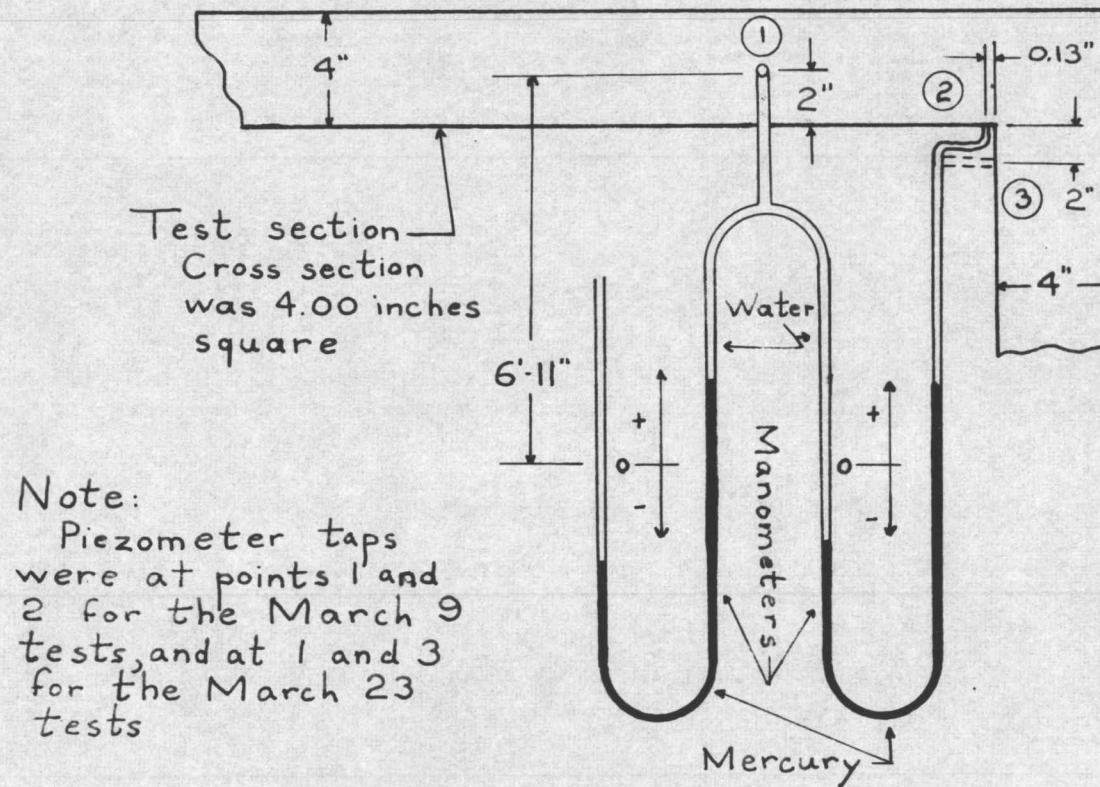


Figure 5

Schematic Diagram of the Laboratory
Test Section Used for the March 9 and
March 23, 1960 Tests

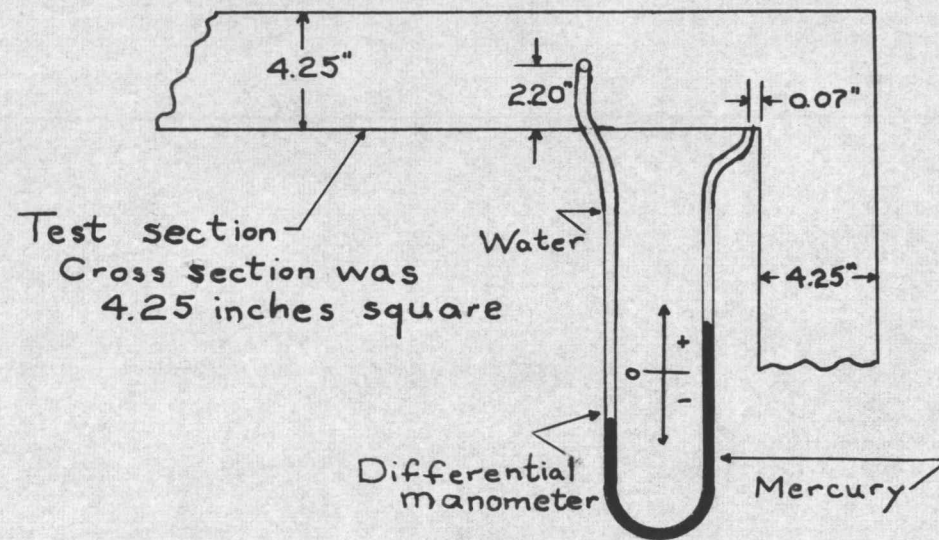


Figure 6

Schematic Diagram of the Laboratory Test Section
Used for the July, 1959 Tests

section is the same as that shown in Figure 5 except that its cross section is 4.25 inches square and the downstream piezometer tap is located closer to the inside corner than is that for the March, 1960, tests.

Procedure

The test section was connected to a surge tank by seventeen feet of ten-inch steel pipe and fifteen feet of five-inch plexiglas pipe. The surge tank was in turn connected to a pump which supplied water from a sump. Flow was regulated by the gate valves indicated in Figure 7. With the valve leading from the tank fully open, the flow was increased by opening the valve leading into the tank. The vertical draft had to be flowing full in order for it to induce cavitation. When the entrance valve was first opened, the draft tube was not flowing full, and the water level in the surge tank rose. As soon as the draft tube was flowing full, on the other hand, the water level started decreasing. This decrease was checked by throttling the exit valve. Steady flow was reached when the surge tank level stayed constant. Different flows were obtained by regulating both valves. The existence of cavitation was determined by the cracking sound made by the formation and collapse of vapor bubbles in the plexiglas conduit.

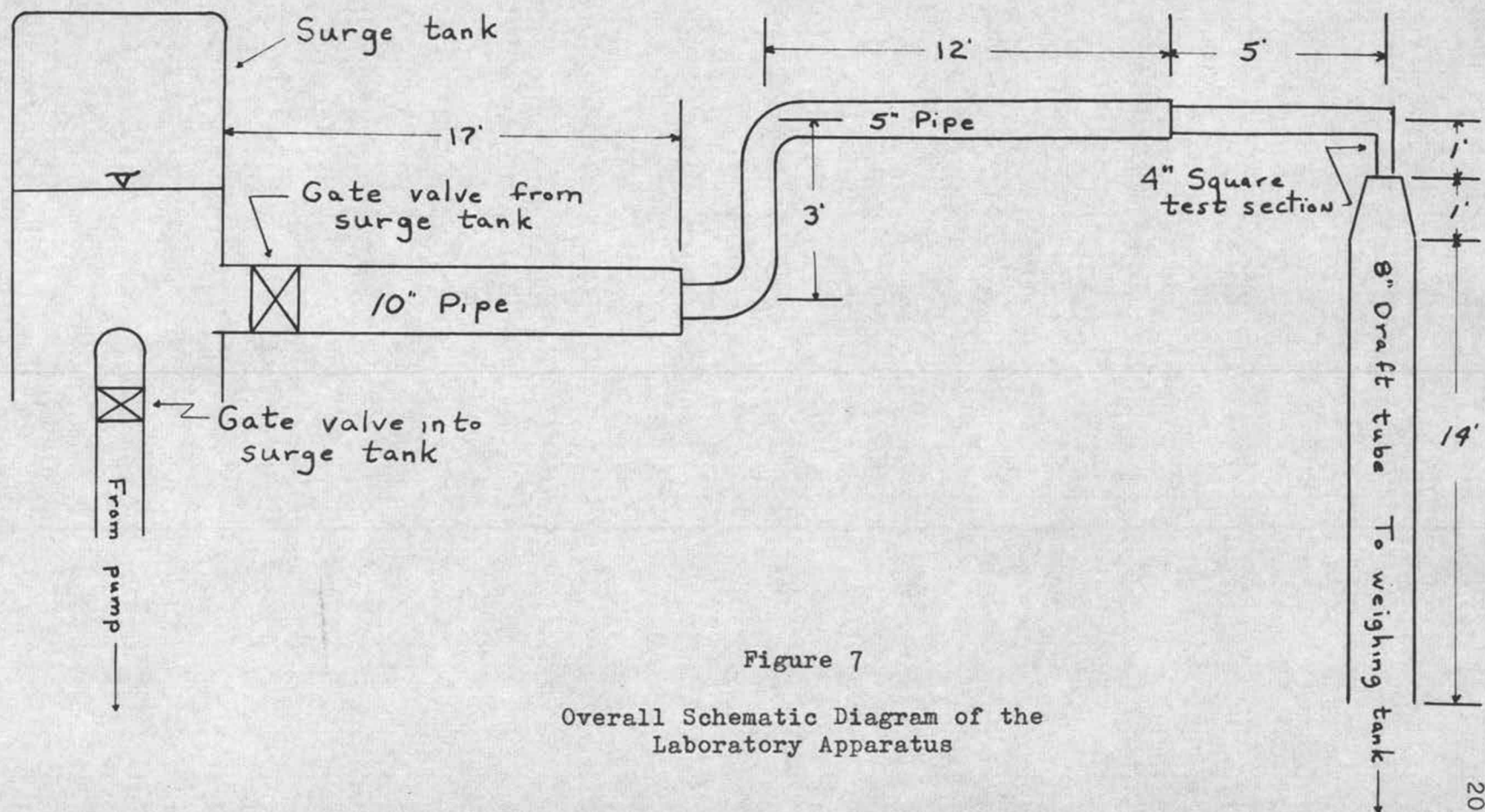


Figure 7

Overall Schematic Diagram of the
Laboratory Apparatus

Calculation of Terms

Average upstream velocity was calculated on the basis of the differences in weighing tank readings after given periods of time. Absolute upstream pressure could be found on the basis of open-end manometer readings, and the difference between absolute upstream and downstream pressures could be calculated on the basis of differential manometer readings.

EXPERIMENTAL RESULTS

A summary of the experimental results is given in Table 2, and the original data is given in Appendix C. As shown in Table 2, the Euler Number is approximately 0.83 when the piezometer is located about an eighth of an inch upstream from the corner, and the parameter is approximately 0.56 when the tap is two inches below the corner on the downstream leg. Also shown here are the absolute pressure heads at the downstream point. The mean values of these pressure heads are approximately +28.5 feet and +15.0 feet when the piezometer is slightly upstream from the corner and two inches downstream from it respectively. Vapor pressure head is 0.83, and so a pressure greater than that of vapor exists at the downstream points measured.

The Euler Number obtained from the Schwartz-Christoffel Transformation is 0.465, which does not agree very closely

TABLE 2

SUMMARY OF EXPERIMENTAL RESULTS

Run #	Mean Euler Number from Laboratory Analysis	Euler Number from Schwartz- Christoffel Transformation	Mean Downstream Pressure Head (feet)	Pressure Head at Vapor Pressure (feet)
March 9, 1960			Absolute Pressures	
1-3	0.826	0.465	28.5	0.83
March 23, 1960				
4-5	0.56	0.465	15.0	0.83
July, 1959				
6-8	0.678	0.465	Absolute Pressures Not Calculated	
9-15	0.683	0.465		

TABLE 2 (Continued)

Notes

1. Assumptions

A. Atmospheric pressure for all tests was the same as that determined for the March 23, 1960 tests, or 32.2 inches of mercury.

$$B. \frac{P_3}{\sigma} = \frac{P_2}{\sigma}$$

2. Differences in Tests

A. Tests dated March 9, 1960 and March 23, 1960 were made using the test section shown in Figure 5. The cross section was four inches square. For the tests dated March 9, 1960, the downstream piezometer was 0.13 inches upstream from the corner, and for those dated March 23, 1960 the tap was two inches below the corner on the downstream leg.

B. Tests dated July, 1959 were made using the test section shown in Figure 6. Cross section was 4.25 inches square, and the downstream piezometer was 0.07 inches upstream from the corner.

3. Existence of Cavitation

For the July, 1959 tests, there was noncavitating flow in runs number 6 through 8, and cavitating flow in runs 9 through 15. Cavitation existed for both sets of March 1960 tests.

with the values obtained from the laboratory analysis. This value does show however, that the pressure at the downstream point is greater than vapor pressure.

CONCLUSIONS

The inconsistency of the theoretical and actual results can be explained by factors that lie in the transformation itself as well as in the laboratory apparatus.

Considering the inside corner of the elbow, where z is zero, the transformation shows the ratio of the velocity at the inside corner to that upstream in the uniform flow section to be infinity. The Euler Number approaches zero and so the difference between the pressure at the corner and that upstream approaches infinity. Therefore, at points near the inside corner the theoretical pressure difference and Euler Number would appear to deviate from the actual quite significantly. Evidently, the point selected for this analysis was too close to the corner. Nevertheless, this point was selected to find the pressure distribution as near as possible to the zone of cavitation.

The Schwartz-Christoffel Transformation assumes non-separating, irrotational flow. In the upstream area analyzed, separation does occur upstream from the outside

corner. (Reference 2, p. 26) This would help to account for the difference in theoretical and actual pressure distribution. As calculated in Appendix D, the Reynolds Number for all the tests was about 500,000. The flows are therefore high enough to yield the velocity distribution demanded by irrotational flow. Nevertheless, the parallel stream lines assumed for irrotational flow are distorted near the boundary because of the fact that the velocity at a smooth boundary surface must be zero. This rotational effect would cause a lower velocity at the downstream point than that calculated by the Schwartz-Christoffel Transformation.

According to flow net theory, the stream lines around the corner of a ninety degree bend follow paths symmetrical about a line joining the inside and outside corners. (Reference 2, p. 24) By centrifugal force however, these stream lines are actually displaced outward from the positions assumed. These inner stream lines force the outer ones inward along the walls, thus setting up a double spiral and reducing the inside pressure. (Reference 3, p. 420)

There are three possibilities for error in the construction of the laboratory apparatus. First, the upstream leg of the test section was not long enough to establish uniform flow. As noted in Appendix D, a length of straight conduit of

approximately seventeen feet is required to establish uniform flow in this section, whereas there were only four feet of square pipe upstream from the point where uniform flow was assumed to exist.

Second, the transition from the five-inch round pipe to the four-inch square pipe produces eddy currents which are carried downstream and which mix the stream lines so that velocity distribution cannot accurately be determined.

For two-dimensional flow, the pipe section should be a rectangle infinitely wide. The third possibility for error then, is that the square cross section does not give this two-dimensional requirement.

The results in Table 2 dated July, 1959 show Euler Numbers that were obtained both with and without cavitation. These parameters are essentially the same, and so the inconsistencies between actual and theoretical results are due to the laboratory conditions and the transformation rather than the presence of cavitation.

The actual conditions that exist in the laboratory analysis therefore only approximate the ideal conditions assumed in the Schwartz-Christoffel Transformation. The scope of this thesis was first to learn about the Schwartz-Christoffel Transformation and the complex variable relations

associated with it, and then to establish a transformation for a two-dimensional mitered elbow, and finally to perform an approximate laboratory analysis of this transformation. A second, more refined, laboratory analysis was therefore not run.

As can be seen in the summary of results, the Euler Numbers derived from the Schwartz-Christoffel Transformation are consistently lower than those determined experimentally. It would therefore appear that if the transformation were applied to any other similar problem, such as a bridge pier, turbine runner, or some other hydraulic shape, results would be in error on the safe side, for actual localized high velocities and local pressure drops would be less than those calculated from the Schwartz-Christoffel Transformation.

BIBLIOGRAPHY

1. Churchill, Ruel V. Introduction to complex variables and applications. New York, McGraw-Hill, 1948. 263 p.
2. Rouse, Hunter. Elementary mechanics of fluids. New York, John Wiley and Sons, 1946. 376 p.
3. Rouse, Hunter. Engineering hydraulics. New York, John Wiley and Sons, 1950. 1039 p.
4. Streeter, Victor L. Fluid dynamics. New York, McGraw-Hill, 1948. 263 p.

APPENDIX

APPENDIX A

Relation of Velocity Ratios to Euler Numbers

Using the Bernoulli Equation between points one and two

$$\frac{V_1^2}{2g} + \frac{p_1}{\sigma} = \frac{V_2^2}{2g} + \frac{p_2}{\sigma}$$

$$\frac{V_2^2}{2g} - \frac{V_1^2}{2g} = \frac{p_1}{\sigma} - \frac{p_2}{\sigma} = \frac{\Delta p}{\sigma} \quad \text{where } V_2 > V_1 \text{ and } p_1 > p_2$$

$$\frac{V_2^2}{V_1^2} - 1 = \frac{\Delta p}{\sigma} \cdot \frac{2g}{V_1^2} = \frac{2 \Delta p}{\rho V_1^2}$$

$$\sqrt{\frac{V_2^2}{V_1^2} - 1} = \frac{\sqrt{\frac{2 \Delta p}{\rho}}}{V_1}$$

$$\frac{1}{\sqrt{\left(\frac{V_2}{V_1}\right)^2 - 1}} = \frac{V_1}{\sqrt{\frac{2 \Delta p}{\rho}}} = \text{Euler Number}$$

APPENDIX B

Finding Values of z , Velocity Ratios,
and Euler Number Using the Schwartz-
Christoffel Transformation Equations

Given $\frac{\phi}{Q} = 0.1910$

Then $\frac{\pi \phi}{Q} = 0.60$

Therefore

$$\frac{\pi \phi}{e^Q} = 1.8221$$

$$\frac{2\pi \phi}{e^Q} = 3.3201$$

$$\frac{-\pi \phi}{e^Q} = 0.5488$$

$$\frac{-2\pi \phi}{e^Q} = 0.3011$$

$$\frac{dw}{dz} \cdot \frac{1}{q} = \sqrt{\frac{\frac{\pi \phi}{e^Q} + 1}{\frac{\pi \phi}{e^Q} - 1}} = 1.8528 = \frac{v_2}{v_1}$$

$$\text{Euler Number} = \frac{1}{\sqrt{\left(\frac{v_2}{v_1}\right)^2 - 1}} = \frac{1}{\sqrt{1.8528^2 - 1}} = 0.638$$

$$\frac{\pi\phi}{e^Q} + \sqrt{\frac{2\pi\phi}{e^Q} - 1} = 1.8221 + 1.5232 = 3.3453$$

$$\ln \left| \frac{\pi\phi}{e^Q} + \sqrt{\frac{2\pi\phi}{e^Q} - 1} \right| = 1.2705$$

$$\frac{-\pi\phi}{e^Q} + \sqrt{\frac{-2\pi\phi}{e^Q} - 1} = 0.5488 + i 0.8359$$

$$\left| \frac{-\pi\phi}{e^Q} + \sqrt{\frac{-2\pi\phi}{e^Q} - 1} \right| = \left| 0.5488 + i 0.8359 \right| = 1.00$$

$$\begin{aligned} \arg \frac{-\pi\phi}{e^Q} + \sqrt{\frac{-2\pi\phi}{e^Q} - 1} &= \arg (0.5488 + i 0.8359) \\ &= \tan^{-1} \frac{0.8359}{0.5488} = 56^\circ 42' 33'' = 0.9899 \end{aligned}$$

$$\begin{aligned} z &= \frac{\ell}{\pi} \left[\ln \left| \frac{\pi\phi}{e^Q} + \sqrt{\frac{2\pi\phi}{e^Q} - 1} \right| + i \arg \frac{\pi\phi}{e^Q} + \sqrt{\frac{2\pi\phi}{e^Q} - 1} \right. \\ &\quad \left. + i \ln \left| \frac{-\pi\phi}{e^Q} + \sqrt{\frac{-2\pi\phi}{e^Q} - 1} \right| - \arg \frac{-\pi\phi}{e^Q} + \sqrt{\frac{-2\pi\phi}{e^Q} - 1} \right] \\ &= \frac{\ell}{\pi} [1.2075 + 0 + 0 - 0.9899] = \frac{\ell}{\pi} (0.2176) \end{aligned}$$

$$\ell = 4.00''$$

$$z = 0.2771''$$

APPENDIX C

Laboratory Results

Original Data

Wednesday, March 9, 1960

Test section as shown in
Figure 3Downstream piezometer at
point z

Barometric Pressure:

29.9 inches--Read
from aneroid baro-
meter which later
proved to be inac-
curate

Run #	Weighing Tank			Manometers			
	Scale Readings		Time Elapsed	Open End		Differential	
	Beginning Pounds	End Pounds	Seconds	Left Inches	Right Inches	Left Inches	Right Inches
1	1000	3500	25	+ 2.7	- 2.4	- 2.4	+ 2.5
2	1000	3500	23	+ 2.4	- 2.0	- 2.9	+ 3.1
3	1000	3500	21	+ 2.1	- 1.7	- 3.5	+ 3.3

Wednesday, March 23, 1960

Test section as shown in
Figure 3Downstream piezometer at
point 3

Barometric Pressure:

32.5 inches absolute
Read from mercury
barometer

Run #	Weighing Tank			Manometers			
	Scale Readings		Time Elapsed	Open End		Differential	
	Beginning Pounds	End Pounds	Seconds	Left Inches	Right Inches	Left Inches	Right Inches
4	1000	3500	23	- 1.5	+ 1.2	- 5.1	+ 5.4
5	1000	3500	21.5	- 1.5	+ 1.4	- 6.0	+ 6.2

Original Data (Continued)

July, 1959

Test section as shown in
Figure 4

Run #	Weighing Tank			Differential Manometer	
	Scale Readings		Time Elapsed		
	Beginning Pounds	End Pounds	Seconds	Left Inches	Right Inches
6	1000	3500	21	- 3.5	+ 3.8
7	1000	3500	20	- 4.1	+ 4.1
8	1000	3500	19	- 4.4	+ 4.3
9	1000	3500	18	- 4.8	+ 4.7
10	1000	3500	17.5	- 5.5	+ 5.4
11	1000	3500	16	- 6.1	+ 6.0
12	1000	3500	15	- 7.4	+ 7.3
13	1000	3500	14.5	- 7.8	+ 7.7
14	1000	3500	14	- 8.1	+ 8.0
15	1000	3500	13	- 10.2	+ 10.0

Sample Calculations

To find V_1

$$\begin{aligned}\text{Water passing through during test period} &= 3500 - 1000 \\ &= 2500\#\end{aligned}$$

$$\text{Time} = 23 \text{ seconds}$$

$$\text{Flow} = \frac{2500}{23} = 108.5 \text{ \#/sec.} = \frac{108.5}{62.4} \text{ \#/cu'} = 1.74 \text{ cfs}$$

$$V_1 = \frac{1.74}{4'' \times 4''} \times 144 \text{ sq''/sq'} = 15.7 \text{ fps}$$

To find p_1

$$\frac{P_{\text{Atmosphere}}}{\sigma_{\text{Hg}}} = 32.5 \text{ inches Hg} = \frac{32.5}{12 \text{ in/ft}} = 2.71 \text{ ft. Hg.}$$

$$= 2.71 \times 13.6 = 36.8 \text{ feet H}_2\text{O}$$

$$\frac{p_1}{\sigma} = \frac{p_A}{\sigma} + \frac{\text{Left Reading} \times 13.6}{12} - \frac{\text{Right Reading} \times 13.6}{12}$$

$$- (6' - 11'' - \frac{\text{Right Reading}}{12})$$

$$= 36.8 + (-1.5 \times \frac{13.6}{12}) - (+1.2 \times \frac{13.6}{12}) - (6.92 - \frac{+1.2}{12})$$

$$= 26.92 \text{ feet}$$

To find p_3

$$\frac{p_3}{\sigma} = \frac{p_1}{\sigma} + \frac{\text{Left Reading}}{12} (13.6 - 1)$$

$$- \frac{\text{Right Reading}}{12} (13.6 - 1) + 4''$$

$$= 26.92 + (-5.1 \times \frac{12.6}{12}) - (+5.4 \times \frac{12.6}{12}) + \frac{4''}{12}$$

$$16.25 \quad \text{Assume this equals } \frac{p_2}{\sigma}$$

$$\begin{aligned} \text{Euler Number} &= \frac{V_1}{\sqrt{\frac{2 \Delta p}{\rho}}} = \frac{V_1}{\sqrt{\frac{2 \Delta p \cdot g}{\sigma}}} = \frac{15.7}{\sqrt{2(26.92 - 16.25) 32.2}} \\ &= \frac{15.7}{26.2} = 0.600 \end{aligned}$$

APPENDIX D

Reynolds Number Calculations

Reynolds Number $N_R = \frac{VD}{\nu}$ for circular pipes of diameter D

Hydraulic radius R of circular pipe = $\frac{\pi D^2}{4} \cdot \frac{1}{\pi D} = \frac{D}{4}$

Therefore

$$N_R = \frac{4VR}{\nu} \text{ for any cross section}$$

For conduit 4 inches square flowing full

$$R = \frac{(4)^2}{4 \cdot 4} = 1 \text{ inch} = 0.0833 \text{ feet}$$

$$V_{\text{minimum}} = 14.45 \text{ fps (Run \#1, Appendix C)}$$

Assume the water temperature is the same as room temperature, or 70° F

$$\nu = 1.05 \times 10^{-5} \text{ ft}^2/\text{sec.}$$

$$N_{R_{\text{minimum}}} = \frac{4 \times 14.45 \times 0.0833}{1.05 \times 10^{-5}} = 4.58 \times 10^5$$

Because Reynolds Number for this analysis was at least 4.52×10^5 , turbulent flow in this test section was quite probable (Reference 2, p. 173), particularly considering upstream disturbances (see Figure 7)

Minimum length for uniform turbulent flow to be established in circular pipe $\approx 50 D$ (Reference 2, p. 189)

For square pipe, minimum length

$$50 (4R) = 200 R$$

$$200 \times 0.0833 = 16.67 \text{ feet}$$